Radiation reaction effects on radiation pressure acceleration

2010 New J. Phys. 12 123005

(http://iopscience.iop.org/1367-2630/12/12/123005)

New Journal of Physics
The open-access journal for physics

Radiation reaction effects on radiation pressure acceleration

M Tamburini[1,4], F Pegoraro[1], A Di Piazza[2], C H Keitel[2] and A Macchi[1,3,4]

[1] Dipartimento di Fisica 'Enrico Fermi', Università di Pisa, Largo Bruno Pontecorvo 3, I-56127 Pisa, Italy
[2] Max-Planck-Institut für Kernphysik, Saupfercheckweg 1, D-69117 Heidelberg, Germany
[3] Istituto Nazionale di Ottica, CNR, Research Unit 'Adriano Gozzini', Pisa, Italy
E-mail: matteo.tamburini@df.unipi.it and andrea.macchi@ino.it

New Journal of Physics **12** (2010) 123005 (14pp)
Received 10 August 2010
Published 7 December 2010
Online at http://www.njp.org/
doi:10.1088/1367-2630/12/12/123005

Abstract. Radiation reaction (RR) effects on the acceleration of a thin plasma foil by a superintense laser pulse in the radiation pressure-dominated regime are investigated theoretically. A simple suitable approximation of the Landau–Lifshitz equation for the RR force and a novel leap-frog pusher for its inclusion in particle-in-cell simulations are provided. Simulations for both linear and circular polarization of the laser pulse are performed and compared. It is found that at intensities exceeding 10^{23} W cm^{-2} the RR force strongly affects the dynamics for a linearly polarized laser pulse, reducing the maximum ion energy but also the width of the spectrum. In contrast, no significant effect is found for circularly polarized laser pulses whenever the laser pulse does not break through the foil.

[4] Authors to whom any correspondence should be addressed.

Contents

1. Introduction

Present-day laser systems may deliver intensities up to $10^{22}\,\mathrm{W\,cm^{-2}}$ [1] at their focal spot. Even higher intensities of the order of 10^{24}–$10^{26}\,\mathrm{W\,cm^{-2}}$ are envisaged at the extreme light infrastructure (ELI). Theoretical studies [2] suggested that in the interaction of a laser pulse with a thin foil, radiation pressure acceleration (RPA) becomes the dominant mechanism of ion acceleration at intensities exceeding $10^{23}\,\mathrm{W\,cm^{-2}}$. The radiation pressure-dominated regime is attractive because of the foreseen high efficiency and because of the quasi-monoenergetic features expected in the ion energy spectrum. Moreover, recent simulations suggest that multi-dimensional effects may allow a further increase of the ion energy [3].

At these extreme optical laser intensities $I \gtrsim 10^{23}\,\mathrm{W\,cm^{-2}}$, electrons become ultra-relativistic within a fraction of the wave period experiencing superstrong accelerations and therefore emitting relatively large amounts of electromagnetic radiation. Radiation reaction (RR) is the influence of the electromagnetic field emitted by each electron on the motion of the electron itself [4] and may become essential under the extreme conditions mentioned above. Early particle-in-cell (PIC) simulations [5] showed that RR effects become important at intensities exceeding $5 \times 10^{22}\,\mathrm{W\,cm^{-2}}$ and increase nonlinearly with the laser intensity.

In order to take RR effects self-consistently into account one should, in principle, solve the so-called Lorentz–Abraham–Dirac (LAD) equation [4]. It is well known that this equation is plagued by inconsistencies such as, for example, the appearance of 'runaway' solutions in which an electron acquires an exponentially diverging acceleration even without any external field. However, it has been shown that in the realm of classical electrodynamics, i.e. neglecting quantum effects, the LAD equation can be consistently approximated by the so-called Landau–Lifshitz (LL) equation, which is free from the mentioned inconsistencies [4, 6].

In this paper, we investigate RR effects in the interaction of a super-intense laser pulse with a thin foil in the RPA-dominant or 'laser-piston' [2] regime by one-dimensional (1D) PIC simulations both for linear and circular polarization. Our approach is based on the LL equation of motion. We identify leading terms in the LL equation and discuss suitable approximations. On the basis of this, we develop a straightforward numerical implementation of the RR force in a standard PIC code. PIC simulations with RR effects included have been previously performed for various laser–plasma interaction regimes by several groups, either using an approach similar to the LL equation [5] or using a different RR modeling [7]–[12].

In our simulations, we check the RR's ability to reduce the electron heating, which is responsible for the broadening of both the electron and ion spectra. Indeed, recent studies for

thick targets in the hole boring regime [11, 12] and ultra-thin plasma slabs [9] suggested that the RR force cools the electrons and may improve the quality of the accelerated ion bunches. We found that in the linear polarization (LP) case, the peak in the energy spectrum has both a lower energy and a lower width when RR is included. At the same time, the fraction of low-energy ions is reduced. However, strong modulations appear in the ion energy spectrum after the acceleration phase both with and without RR and eventually the quasi-monoenergetic features are lost. In the circular polarization (CP) case, RR does not affect the ion energy spectrum significantly even at intensities of the order of $10^{24}\,\mathrm{W\,cm^{-2}}$. The differences between LP and CP appear to be related to the longitudinal electron oscillations driven by the $\mathbf{J}\times\mathbf{B}$ force in the LP case. These oscillations allow a deeper penetration of the laser pulse into the foil enhancing the effect of the RR force on electrons. In the CP case, significant RR effects are found only for laser and target parameters such that the laser pulse breaks through the foil due to nonlinear transparency, similar to what was found in previous studies [9].

2. The radiation reaction force

In classical electrodynamics, the effect of RR on the motion of an electron can be included by means of an additional force besides the Lorentz force. The additional RR force basically describes the loss of energy and momentum by an accelerated electron that radiates EM waves, so that the electron trajectory changes with respect to that predicted by the Lorentz force alone. In the LL approach [4], the RR force is written in a manifestly covariant form as

$$f^{\mu}=\frac{2e^{3}}{3mc^{2}}\left(\partial_{\alpha}F^{\mu\nu}u_{\nu}u^{\alpha}\right)+\frac{2e^{4}}{3m^{2}c^{4}}\left(F^{\mu\nu}F_{\nu\alpha}u^{\alpha}+(F^{\nu\beta}u_{\beta}F_{\nu\alpha}u^{\alpha})u^{\mu}\right), \tag{1}$$

where m and e are the electron mass and charge, respectively, $u^{\mu}=(\gamma,\,\gamma\mathbf{v}/c)$ is its four-velocity and $F^{\mu\nu}$ is the electromagnetic tensor relative to the total electromagnetic field acting on the electron except for the field generated by the electron itself.

The importance of RR effects on the electron motion depends on the strength and geometry of the EM fields, as well as on the electron energy, which is generally a function of the amplitude and frequency of the field itself. One would thus need to know at least the scaling of the electron energy with the laser pulse parameters for a preliminary evaluation of RR effects as well as for a discussion of the limits of validity of the chosen theoretical approach and of suitable approximations to it. In the following discussion, we mostly refer to the case of electron motion in a plane wave. For this problem, the LL equation has an exact analytical solution for arbitrary pulse shape and polarization of the plane wave [13]. Such a solution thus provides a useful benchmark and reference for RR effects in superstrong laser fields. In a many-particle system such as a high-density plasma, the collective EM fields are generally much more complicated but the plane wave results may provide some guidance for their interpretation.

We first recall that the LL approach is classical and quantum electrodynamic effects are neglected. In the interaction between an intense laser field (with peak intensity I and wavelength λ) and an ultra-relativistic electron (with Lorentz factor of the order of γ) this is in general allowed if $\gamma\sqrt{I/I_{\mathrm{cr}}}\ll 1$ and $\gamma\lambda_{\mathrm{c}}/\lambda\ll 1$ [4], where $I_{\mathrm{cr}}=cE_{\mathrm{cr}}^{2}/8\pi\approx 2.3\times 10^{29}\,\mathrm{W\,cm^{-2}}$ is the intensity corresponding to the critical field $E_{\mathrm{cr}}=m^{2}c^{3}/\hbar|e|$ of quantum electrodynamics [14] and $\lambda_{\mathrm{c}}=\hbar/mc\approx 3.9\times 10^{-7}\,\mu\mathrm{m}$ is the Compton wavelength. These conditions ensure that the momentum of the photons emitted or absorbed by the electron is negligible. Moreover, the force related to the electron spin might not be negligible in comparison

to the RR force. In fact, the dynamics of a particle with a spin degree of freedom in an external electromagnetic field can be described in the classical framework by the Frenkel force [15] (see also [16] for a different derivation of both the RR and the spin force)

$$f_{\mathrm{S}}^{\mu} = -\tfrac{1}{2} Q^{\gamma\delta} \partial^{\mu} F_{\gamma\delta} + \tfrac{1}{2} (Q^{\gamma\delta} \partial_{\lambda} F_{\gamma\delta} u^{\lambda}) u^{\mu}, \tag{2}$$

where $Q^{\gamma\delta} = \varepsilon^{\gamma\delta\alpha\beta} u_{\alpha} m_{\beta}$, m^{α} is the magnetic dipole moment four-vector and $\varepsilon^{\gamma\delta\alpha\beta}$ is the Levi-Civita symbol ($\varepsilon^{0123} = +1$). The analysis of the case of a plane wave (electric field amplitude E, central frequency ω and pulse length τ) shows that the spin force is $\sim \gamma/\alpha \simeq 137\gamma$ times the term in the LL force (1) containing the derivatives of the field tensor, i.e. the term proportional to $\partial_{\lambda} F^{\mu\nu}$ (here $\alpha = e^2/\hbar c \approx 1/137$ is the fine-structure constant). However, it can also be shown that the spin effects remain smaller than those due to the last term in equation (1) if $\alpha a_0 \omega \tau \gtrsim 1$ where $a_0 = |e|E/m\omega c$ (the effect of the last RR term cumulates with time). Since $\tau > 2\pi/\omega$ and $a_0 > 300$ in our simulations the latter condition is well satisfied. It is therefore consistent, in a regime where RR effects are relevant and quantum effects are subdominant, to neglect both the spin force and the first term of the RR force in equation (1).

The PIC simulations with the RR force included are performed in the laboratory frame, i.e. the frame where the plasma target is initially at rest. In the laboratory frame, we write down the LL equation in a 3D, non-manifestly covariant form as

$$\begin{aligned} \frac{\mathrm{d}\mathbf{p}}{\mathrm{d}t} = &-(\mathbf{E} + \mathbf{v} \times \mathbf{B}) - \left(\frac{4}{3}\pi \frac{r_{\mathrm{e}}}{\lambda}\right) \gamma \left[\left(\frac{\partial}{\partial t} + \mathbf{v} \cdot \nabla\right) \mathbf{E} + \mathbf{v} \times \left(\frac{\partial}{\partial t} + \mathbf{v} \cdot \nabla\right) \mathbf{B}\right] \\ &+ \left(\frac{4}{3}\pi \frac{r_{\mathrm{e}}}{\lambda}\right) [(\mathbf{E} + \mathbf{v} \times \mathbf{B}) \times \mathbf{B} + (\mathbf{v} \cdot \mathbf{E})\mathbf{E}] - \left(\frac{4}{3}\pi \frac{r_{\mathrm{e}}}{\lambda}\right) \gamma^2 [(\mathbf{E} + \mathbf{v} \times \mathbf{B})^2 - (\mathbf{v} \cdot \mathbf{E})^2] \mathbf{v}, \end{aligned} \tag{3}$$

where $\mathbf{p}$ is the electron momentum, $r_{\mathrm{e}} \equiv e^2/mc^2 \approx 2.8 \times 10^{-9}\,\mu$m is the classical electron radius, $\lambda = 2\pi c/\omega$ is the laser wavelength and we use dimensionless quantities as in the PIC code. Time is normalized in units of ω^{-1}, space in units of $c\omega^{-1}$ and momenta in units of mc. Consequently, EM fields are normalized in units of $m\omega c/|e|$ and densities in units of the critical density $n_{\mathrm{c}} = m\omega^2/4\pi e^2$. The first RR term of equation (3), i.e. the one containing the 'total' time derivative of the EM fields, corresponds to the negligible term in the manifestly covariant LL equation (1) and is reported here for completeness but neglected in the calculations for the above-explained reasons.

Since RR effects are important for ultra-relativistic electrons $\gamma \gg 1$, the last term in equation (3) (proportional to γ^2) dominates over the preceding one. From a practical point of view, the smaller term may often be neglected even though the on-shell condition $u_{\mu} u^{\mu} = 1$ is lost neglecting this term. Although single particle and PIC tests with and without this term showed no significant difference, both terms were included in our PIC simulations. It is possibly instructive, however, to neglect for a moment the smaller term and write down an effective reduced LL equation in the *laboratory frame*

$$\frac{\mathrm{d}\mathbf{p}}{\mathrm{d}t} = \mathbf{f}_{\mathrm{L}} - d\mathbf{v}, \tag{4}$$

where $\mathbf{f}_L \equiv -(\mathbf{E} + \mathbf{v} \times \mathbf{B})$ and d is given by

$$\begin{aligned} d &\equiv \left(\frac{4}{3}\pi \frac{r_{\mathrm{e}}}{\lambda}\right) \gamma^2 [\mathbf{E}^2 - (\mathbf{v} \cdot \mathbf{E})^2 + \mathbf{v}^2 \mathbf{B}^2 - (\mathbf{v} \cdot \mathbf{B})^2 - 2\mathbf{v} \cdot (\mathbf{E} \times \mathbf{B})] \\ &= \left(\frac{4}{3}\pi \frac{r_{\mathrm{e}}}{\lambda}\right) \gamma^2 [\mathbf{f}_{\mathrm{L}}^2 - (\mathbf{v} \cdot \mathbf{f}_L)^2] \geqslant 0. \end{aligned} \tag{5}$$

In equation (4), RR effects appear as a 'friction' term with a nonlinear and anisotropic friction coefficient given by d. When an electron 'crosses' an EM field, it feels a viscous force opposite to its velocity.

For an ultra-relativistic electron, the friction coefficient d may be used as a measure of the strength of the RR force in units of $m\omega c$. In the case of motion in a plane wave, d may be compared directly to the normalized wave amplitude a_0. Setting $\mathbf{E} \times \mathbf{B}$ along the positive x-axis, the RR force vanishes ($d \to 0$) when $v_x \to 1$, has its maximum value ($d \to (\frac{4}{3}\pi \frac{r_e}{\lambda})\gamma^2 4a_0^2$) when $v_x \to -1$ and, finally, $d \to (\frac{4}{3}\pi \frac{r_e}{\lambda})\gamma^2 a_0^2$ when $(v_y^2 + v_z^2) \to 1$.

The friction effect of the RR physically corresponds to the incoherent emission of high-frequency radiation by ultra-relativistic electrons. When the RR is included in the numerical simulation of a collisionless, relativistic plasma, it is typically not feasible to resolve electromagnetic waves at such high frequencies, much larger than the inverse of the temporal resolution. Thus, it is assumed that such radiation escapes from the system without re-interacting with other electrons. Note that even a solid-density plasma is transparent to such radiation, since in the present regime the RR effect is mostly due to the emission of radiation with photon energies in the MeV range, while the plasma frequency corresponds to at most a few hundreds of eV. From the point of view of energy balance then, the energy radiated at high frequencies appears as a loss term or 'dissipation'. The percentage of radiative loss is measured by comparing the energy balance simulations including RR with simulations without RR, where the total energy of fields and particles is conserved within the limits of numerical accuracy (typically within 1% in our PIC code).

It may be worth recalling that, for what concerns the LL equation of motion, energy and momentum are not conserved exactly for the single electron. This is due to some terms that are neglected when deriving the LL equation from the LAD equation under the assumption that the radiation force in the instantaneous rest frame of the electron is much smaller than the Lorentz force [4]. However, the neglected terms are much smaller than quantum corrections [4]; thus the approximation is consistent with a classical treatment. In a different approach to the RR force recently presented in [17], a different couple of classical equations of motion are derived phenomenologically starting from the requirement of energy–momentum conservation of the system of the electromagnetic field plus the radiating electron.

3. The numerical approach

Our PIC code is based on the standard, widely used Boris particle pusher [18] and leap-frog schemes to advance and accelerate particles. We developed a simple numerical scheme to insert the RR force in the PIC code while keeping the standard particle pusher for the Lorentz force unchanged. As will be clear below, this scheme is based on the assumption that the acceleration of particles is dominated by the Lorentz force, with the RR force giving a smaller, albeit non-negligible contribution.

We write the total force $\mathbf{f}$ acting on the electron as the sum of two forces $\mathbf{f}_L$ (already introduced) and $\mathbf{f}_R$, with

$$\mathbf{f}_R = -\left(\frac{4}{3}\pi \frac{r_e}{\lambda}\right)\left\{\mathbf{f}_L \times \mathbf{B} - (\mathbf{v}\cdot\mathbf{E})\mathbf{E} + \gamma^2\left[\mathbf{f}_L^2 - (\mathbf{v}\cdot\mathbf{E})^2\right]\mathbf{v}\right\}. \tag{6}$$

Then, the equation of motion of the electron reads

$$\frac{\mathrm{d}\mathbf{p}}{\mathrm{d}t} = \mathbf{f} = \mathbf{f}_L + \mathbf{f}_R. \tag{7}$$

Assuming that forces and momenta are known at integer and half-integer timesteps respectively, the full leap-frog step is

$$\frac{\mathbf{p}^{(n+1/2)} - \mathbf{p}^{(n-1/2)}}{\Delta t} = \mathbf{f}^{(n)} = \mathbf{f}_{\mathrm{L}}^{(n)} + \mathbf{f}_{\mathrm{R}}^{(n)}, \tag{8}$$

where Δt is the timestep. Now, we consider the leap-frog step for two 'helper' momenta $\mathbf{p}_{\mathrm{L}}$ and $\mathbf{p}_{\mathrm{R}}$

$$\frac{\mathbf{p}_{\mathrm{L}}^{(n+1/2)} - \mathbf{p}_{\mathrm{L}}^{(n-1/2)}}{\Delta t} = \mathbf{f}_{\mathrm{L}}^{(n)}, \quad \frac{\mathbf{p}_{\mathrm{R}}^{(n+1/2)} - \mathbf{p}_{\mathrm{R}}^{(n-1/2)}}{\Delta t} = \mathbf{f}_{\mathrm{R}}^{(n)} \tag{9}$$

and assume $\mathbf{p}_{\mathrm{L}}^{(n-1/2)} = \mathbf{p}_{\mathrm{R}}^{(n-1/2)} = \mathbf{p}^{(n-1/2)}$. Thus, from the above equations we easily obtain

$$\mathbf{p}^{(n+1/2)} = \mathbf{p}_{L}^{(n+1/2)} + \mathbf{p}_{R}^{(n+1/2)} - \mathbf{p}^{(n-1/2)}. \tag{10}$$

This means that, starting at time $t^{(n)}$ and position $\mathbf{x}^{(n)}$ with $\mathbf{p}^{(n-1/2)}$, firstly $\mathbf{p}_{\mathrm{L}}^{(n+1/2)}$ and $\mathbf{p}_{\mathrm{R}}^{(n+1/2)}$ are calculated *independently* using $\mathbf{f}_{\mathrm{L}}^{(n)}$ and $\mathbf{f}_{\mathrm{R}}^{(n)}$, respectively, and finally equation (10) is employed to obtain the full leap-frog step $\mathbf{p}^{(n+1/2)}$. It is worth noting that this is a general result as we have used only the superposition property of the force without any assumption about $\mathbf{f}_{\mathrm{L}}$ and $\mathbf{f}_{\mathrm{R}}$.

The previous algorithm allows us to keep the standard leap-frog pusher for the Lorentz force and to develop an independent pusher for the RR force alone. Using equation (9) we can recast equation (10) as

$$\mathbf{p}^{(n+1/2)} = \mathbf{p}_{\mathrm{L}}^{(n+1/2)} + \mathbf{f}_{\mathrm{R}}^{(n)} \Delta t = \mathbf{p}_{\mathrm{R}}^{(n+1/2)} + \mathbf{f}_{\mathrm{L}}^{(n)} \Delta t. \tag{11}$$

Now, in order to compute the momentum change from step $n - 1/2$ to $n + 1/2$ due to the Lorentz and the RR force, an estimate of the electron's velocity at half-step n is needed. To this aim, we first advance $\mathbf{p}^{(n-1/2)}$ to $\mathbf{p}_{\mathrm{L}}^{(n+1/2)}$ using the Boris pusher for the Lorentz force, and then we use $\mathbf{p}_{\mathrm{L}}^{(n+1/2)}$ to estimate the *total* momentum $\mathbf{p}^{(n)}$ and velocity $\mathbf{v}^{(n)}$ at half timestep as

$$\mathbf{p}^{(n)} \approx \frac{\mathbf{p}_{\mathrm{L}}^{(n+1/2)} + \mathbf{p}^{(n-1/2)}}{2}; \quad \mathbf{v}^{(n)} \approx \frac{\mathbf{p}^{(n)}}{\gamma^{(n)}}, \tag{12}$$

where

$$\gamma^{(n)} = \sqrt{1 + (\mathbf{p}^{(n)})^2}. \tag{13}$$

Next, we use equations (12) and (13) together with the fields $\mathbf{E}^{(n)}$ and $\mathbf{B}^{(n)}$ at half timestep to compute the full term $\mathbf{f}_{\mathrm{R}}^{(n)}$ according to equation (6). This task is particularly simple because many terms of $\mathbf{f}_{\mathrm{R}}$ can be written by $\mathbf{f}_{\mathrm{L}}$ directly (see equation (6)).

This particle pusher was tested comparing the numerical results for a single electron in a monochromatic plane wave both with the known analytical solution [13] and with the numerical solution obtained using a fourth-order Runge–Kutta scheme. These numerical calculations confirmed that the inclusion of the RR force according to the above method preserves the accuracy and stability of the standard Boris pusher algorithm. The range of intensities in the tests was from 10^{22} to $10^{24}\,\mathrm{W\,cm^{-2}}$ with $\lambda = 0.8\,\mu$m. Taking as an example case an electron with initial momentum $p_{x_0} = -200\,mc$ and a wave with $a_0 = 350$ and $\lambda = 0.8\,\mu$m, we found our particle pusher to yield a phase error in the longitudinal momentum of $\sim 10^{-2}(2\pi)$ after a runtime of $500\omega^{-1}$ using a timestep $\Delta t = 0.01\omega^{-1}$. The corresponding relative error in the displacement in the direction of wave propagation was $\sim 4 \times 10^{-4}$. The one-particle tests were performed using the complete expression for the LL force (3) with the fields and their derivatives

as given functions of space and time. These tests also confirmed that the derivative term in the LL force (3) is negligible. The inclusion of the RR force in the PIC code according to the above-described approach leads to an approximately 10% increment of the computing time.

4. The particle-in-cell (PIC) simulations

We performed PIC simulations with a plasma slab of ions (protons) with uniform initial density n_0. Since our primary aim is to evaluate the importance of RR effects on laser–plasma dynamics and ion acceleration in the regime of radiation pressure dominance, we restrict ourselves to a 1D geometry for the sake of simplicity and the possibility of using high numerical resolution. Multi-dimensional effects, which may be important to determine the features of ion acceleration in this regime [3], will be presented in forthcoming publications; preliminary 2D simulations [19] show qualitatively similar trends to the 1D case. It is worth noting that, as the momentum space in the 1D PIC code is already 3D, our numerical approach can be readily implemented in a multi-D code employing the same particle pusher. The modest increase in computational time implied by our method might be essential to be able to perform large-scale multi-D simulations with RR included.

We report results for a laser intensity $I = 2.33 \times 10^{23}\,\mathrm{W\,cm^{-2}}$ and a laser wavelength $\lambda = 0.8\,\mu\mathrm{m}$, corresponding to a dimensionless parameter $a_0 = 328$. In all the simulations, the density $n_0 = 100 n_c$ and the profile of the laser field amplitude has a 'trapezoidal' shape in time with one-cycle, $\sin^2$-function rise and fall and a five-cycle constant plateau. The laser pulse front reaches the edge of the plasma foil at $t = 0$. The foil thickness is $\ell = 1\lambda$ in all the simulations except for the 'transparency' case reported below, for which $\ell = 0.3\lambda$. We considered both CP and LP of the laser pulse. The parameters are similar to those of the 3D simulations in [2], where the laser pulse was linearly polarized. According to [2], RPA dominates the acceleration of ions in the plasma foil when the laser intensity $I \gtrsim 10^{23}\,\mathrm{W\,cm^{-2}}$. To our knowledge, neither RR effects nor CP have been studied so far in such a regime of laser and plasma parameters. The effects of CP have been studied extensively at lower intensities (see e.g. [20] and references therein), showing that, with respect to LP, the use of CP quenches the generation of highly relativistic electrons, making RPA dominant also at such lower intensities. Concerning RR effects, in [2] it was suggested that the higher the velocity to which the plasma foil is accelerated, the lower the RR force becomes, because of the relativistic increase of the laser wavelength λ' in the foil frame, making the RR strength parameter $\sim r_e/\lambda'$ increasingly small. The expected quenching of RR effects may also be explained with the help of the 'reduced' LL equations (4) and (5): when the foil moves coherently with a velocity close to c, the amplitude of the reflected wave is strongly reduced at any time in the laboratory frame; thus, the electrons at the surface of the foil can be considered as moving with a velocity $v_x \simeq c$ in the field of the incident plane wave and parallel to its propagation direction, and the RR force almost vanishes.

In the CP case, we found that RR effects on the ion spectrum (distribution of protons per unit energy) are negligible as shown in figure 1 for a time $t = 46T$ where $T = \lambda/c$ is the laser period. Even at higher intensities, RR effects on the ion spectrum are weak provided that there is not a strong transmission of the laser pulse through the foil. In the simulation corresponding to figure 1, the laser pulse penetrates into the plasma for a small distance of the order of $\lambda/20$, and the fields in the plasma are much smaller than the fields in vacuum. As a consequence, the friction coefficient d introduced in equation (5) is very small compared to a_0. The spatial profiles of both the fields and the coefficient d in the 'skin' layer are shown in figure 2. The

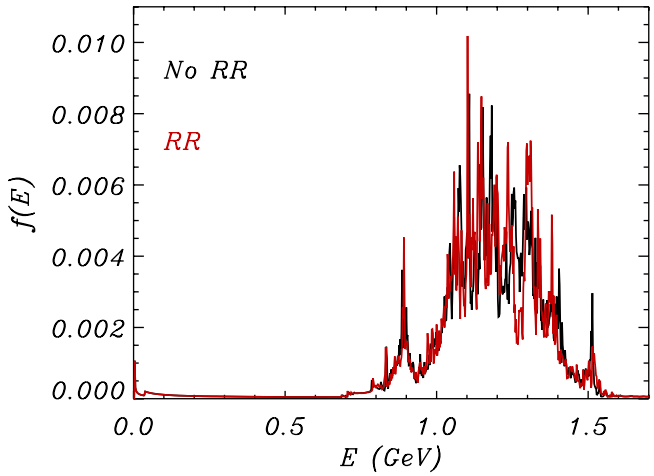

Figure 1. Ion energy spectrum $f(E)$ at $t = 46\,T$ with (red) and without (black) RR for CP. The laser intensity is $I = 2.33 \times 10^{23}\,\mathrm{W\,cm^{-2}}$ and the target thickness is $\ell = 1\lambda$. See the text for the parameters common to all the simulations.

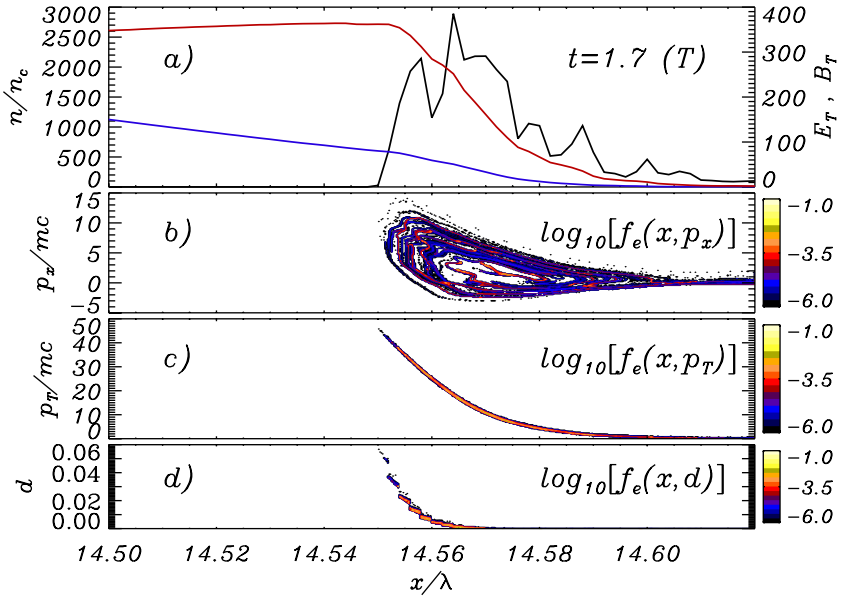

Figure 2. Snapshot at $t = 1.7\,T$ of the 'skin' layer of the foil for CP and $I = 2.33 \times 10^{23}\,\mathrm{W\,cm^{-2}}$. The foil was initially placed between $x = 14\lambda$ and $x = 15\lambda$. (a) The electron density (black), the modulus of the transverse electric $E_\perp = \sqrt{E_y^2 + E_z^2}$ (blue) and magnetic $B_\perp = \sqrt{B_y^2 + B_z^2}$ (red) fields. Distribution of (b) the longitudinal momentum p_x, (c) modulus of the transverse momentum $p_\perp = \sqrt{p_y^2 + p_z^2}$ and (d) friction coefficient d.

order of magnitude of the normalized transverse momentum is $\mathbf{p}_\perp \sim 10$ and that of the friction coefficient is $d \sim 10^{-2}$. It is worth mentioning that figure 2 shows a snapshot at $t = 1.7\,T$, but the typical values of the friction coefficient d are always of the same order of magnitude for CP. In contrast, for LP the friction coefficient d attains much larger values at the same instant,

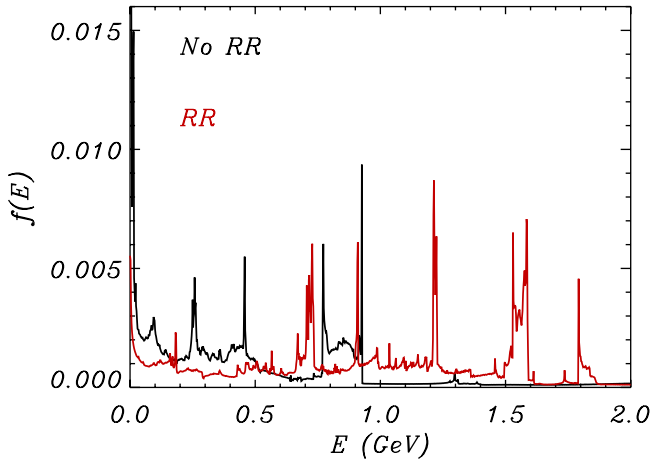

Figure 3. Ion energy spectrum $f(E)$ at $t = 46\,T$ for a simulation with the same parameters as figure 1 but with a target thickness $\ell = 0.3\lambda$. In this case, the laser pulse breaks through the foil and RR effects are evident.

as discussed below. We also note that, for CP, we obtain qualitatively similar results also at higher intensities, up to $10^{24}\,\mathrm{W\,cm^{-2}}$. However, at such extremely high intensities the condition of validity of the classical approach ($\gamma\sqrt{I/I_{\mathrm{cr}}} < 1$) tends to be violated, so at least such results should be taken with caution and an analysis based on quantum RR effects might be necessary.

Reducing the foil density or thickness, the laser pulse may break through the foil. In this case more electrons move in a strong electromagnetic field becoming ultra-relativistic in a fraction of the wave cycle and RR effects strongly affect the ion spectrum, as shown in figure 3. In particular, when RR is included, peaks in the energy spectrum appear at energies higher than in the case without RR. This result is similar to that obtained in [9] at lower intensities ($\sim 10^{22}\,\mathrm{W\,cm^{-2}}$), where it was suggested that RR effects 'improve' the ion spectrum in the optical transparency regime. Our explanation is that the effective 'dissipation' due to RR leads to a later breakthrough of the laser pulse through the foil, favoring a longer and more efficient RPA stage. However, comparing figure 3 with the thicker target case in figure 1, it is evident that the spectrum becomes very far from monoenergetic, while the maximum ion energy increases only slightly. Hence, in our simulations 'optimal' conditions for ion acceleration are found for the case of figure 1; for the corresponding laser and plasma parameters, RR effects are negligible.

In the LP case, the foil is accelerated by radiation pressure too but unlike the CP case, the laser pulse does penetrate up to a fraction of the order of $\lambda/4$ at the front surface of the foil, as shown in figure 4. The two snapshots are selected both to show values of d close to its maximum in time and to make a direct comparison with the CP case of figure 2. It is found that a larger fraction of electrons at the front surface move in a strong electromagnetic field of the same order as the vacuum fields. In this case, the friction coefficient function d reaches values of $d \approx 10^2$ (figure 4), which are comparable with the Lorentz force ($a_0 = 328$). The deeper penetration of the laser pulse is correlated with the strong longitudinal oscillatory motion driven by the oscillating component of the $\mathbf{J} \times \mathbf{B}$ force, which is suppressed for CP. Large numbers of electrons are pushed periodically inside the foil, producing strong fluctuations of the electron density (see figure 4, part (a)).

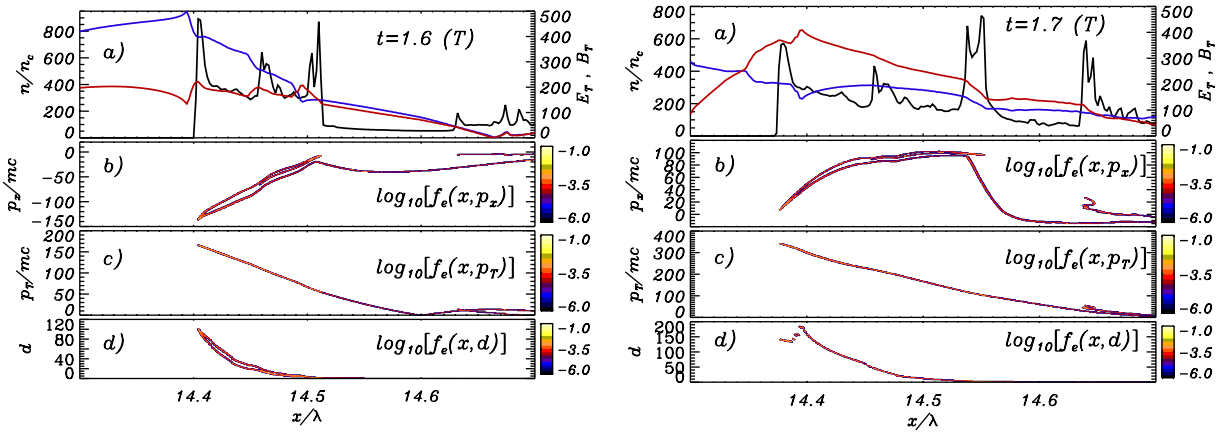

Figure 4. Snapshot at $t = 1.6\,T$ and $t = 1.7\,T$ of the 'skin' layer of the foil for LP and $I = 2.33 \times 10^{23}\,\mathrm{W\,cm^{-2}}$. The strong longitudinal oscillations driven by the $\mathbf{J} \times \mathbf{B}$ force allow a deeper penetration of the laser pulse into the foil compared to the CP case. The foil was initially placed between $x = 14\lambda$ and $x = 15\lambda$. (a) The electron density (black), the modulus of the transverse electric $|E_y|$ (blue) and magnetic $|B_z|$ (red) fields. Distribution of (b) the longitudinal momentum p_x, (c) modulus of the transverse momentum $p_\perp = |p_y|$ and (d) friction coefficient d. Note the change of the scale from $t = 1.6\,T$ and $t = 1.7\,T$ in frames (b), (c) and (d). We remark that the values of the longitudinal momentum p_x vary by orders of magnitude within a time $0.1\,T$ due to the $\mathbf{J} \times \mathbf{B}$ force.

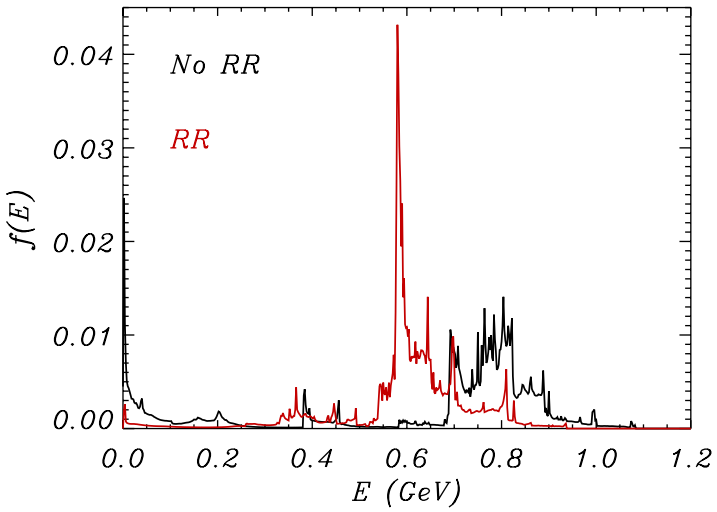

Figure 5. Ion energy spectrum at $t = 12\,T$ with (red) and without (black) RR for LP and $I = 2.33 \times 10^{23}\,\mathrm{W\,cm^{-2}}$.

For LP, the ion energy spectrum is significantly affected by RR effects. The spectrum is fairly peaked with a *smaller* energy spread and a *lower* peak energy than in the case without RR (figure 5). In general, as observed in many simulations, the spectral peak produced by RPA broadens with increasing electron 'temperature', since hot electrons drive the expansion of the

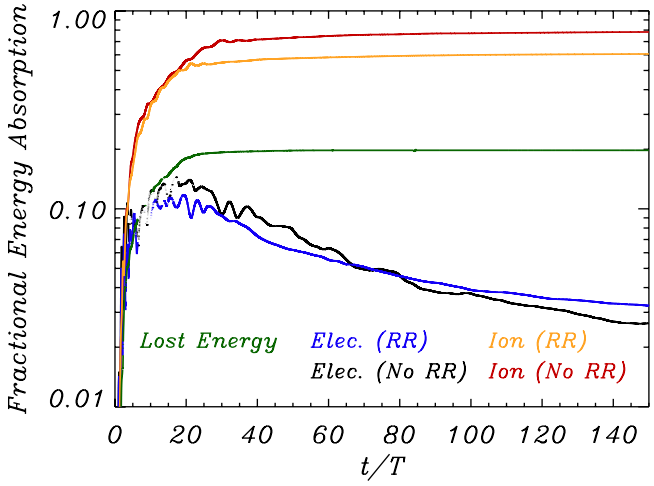

Figure 6. Fractional energy absorption as a function of time for LP and intensity $I = 2.33 \times 10^{23}\,\mathrm{W\,cm^{-2}}$. Electron kinetic energy with RR (blue) and without RR (black), ion kinetic energy with RR (orange) and without RR (red) and the fraction of energy lost in the system (green).

plasma, leading to additional, non-monoenergetic ion acceleration. The smaller energy spread observed when RR is included can thus be traced back to the radiative cooling of the most energetic electrons. Moreover, a significant fraction of ions on the low-energy tail of the spectrum are observed in the case without RR, but disappear when RR is included. The fractional difference in ion energy with RR versus without RR is of the order of the fraction of the laser pulse energy that is 'lost' as incoherent emission (figure 6). For $I = 2.33 \times 10^{23}\,\mathrm{W\,cm^{-2}}$, about 20% of the total pulse energy is lost as incoherent radiation (figure 6).

When RR is 'switched off', part of the 'skin' layer of the foil is left behind and a significant fraction of ions are present in the low-energy tail of the ion spectrum (figure 5). To explain this effect, we first recall that in the first stage of RPA two ion populations may be produced, corresponding to a coherently moving 'sail' and to a trailing 'tail' [20]. Ions in the tail will eventually remain behind the sail if their charge is neutralized by returning electrons; otherwise, they will be accelerated by their own space-charge field and may move to the higher energy side. When the foil is still non-relativistic in the laboratory frame, the RR force has larger values when the electrons counterpropagate with respect to the laser pulse and therefore the electron backward motion is strongly impeded when the RR force is included. This effect prevents an efficient neutralization of the ion charge in the tail by returning electrons, explaining why a higher number of low-energy ions are observed without RR.

Equation (4) suggests that the RR force is mainly a nonlinear friction force. For $I = 2.33 \times 10^{23}\,\mathrm{W\,cm^{-2}}$, about 20% of the total pulse energy is 'dissipated' by the RR force during the laser–foil interaction (figure 6), which lasts about 22 cycles (30 cycles without RR). As stated previously, such 'dissipated' energy accounts for the incoherent radiation escaping from the plasma. During the laser–foil interaction, such a flux of incoherent radiation shows itself in a missing pulse energy, while ions have almost the same total energy in both cases and their spectrum is quasi-monochromatic (figure 5). However, after the acceleration phase by the radiation pressure of the laser pulse, a 20% missing pulse energy implies nearly the same

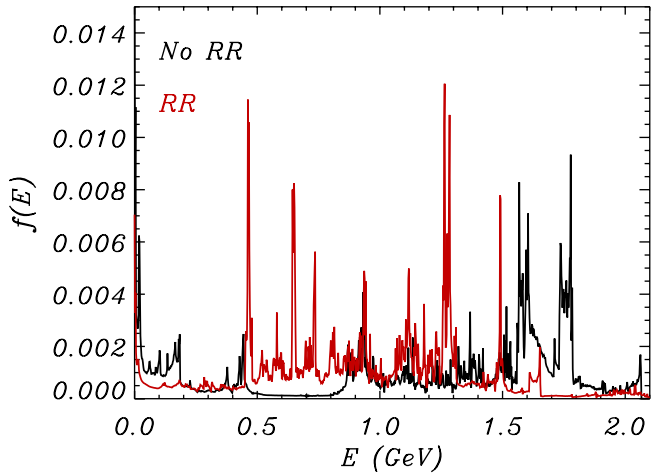

Figure 7. Ion energy spectrum at $t = 46\,T$ with (red) and without (black) RR for LP and $I = 2.33 \times 10^{23}\,\mathrm{W\,cm^{-2}}$.

amount of missing final ion energy (figure 6). Moreover, a significant fraction of hot electrons are produced by the $\mathbf{J} \times \mathbf{B}$ force. Such electrons can drive an expansion of the foil, strongly increasing the ion energy spread after the laser–foil interaction phase (figure 7).

We remark that just changing the laser polarization from CP to LP, the friction coefficient d increases by up to four orders of magnitude due the enhanced laser pulse penetration into the foil by the $\mathbf{J} \times \mathbf{B}$-driven longitudinal oscillations. Then, the electrons move in a strong electromagnetic field becoming ultra-relativistic and the 'friction' term of the RR force becomes non-negligible. These results are a relevant test of the conjecture in [2] that RR effects would be weak as the foil motion becomes relativistic. Our simulations suggest that this picture strictly holds only in the CP case, where almost all of the foil moves at relativistic speed in the same direction as the laser pulse. In the LP case, a substantial fraction of electrons has both an ultra-relativistic motion in the transverse direction and a strong oscillatory motion in the longitudinal direction, leading to significant RR effects.

The dependence of RR effects on the pulse polarization was also studied in [10]–[12] for thick targets ('hole boring' regime of RPA) and long pulse durations. It was also found that RR effects are stronger for LP, although they are not negligible for CP [12]. These results cannot be compared straightforwardly to our findings because of the quite different laser and plasma parameters, leading to different dynamics. For instance, in the thick target case the laser–plasma surface oscillates also for CP ('piston oscillations' [12]) and a return current of electrons counterpropagating with respect to the laser pulse is generated; this effect is likely to enhance radiative loss.

5. Conclusions

We summarize this work as follows. Radiation reaction effects on radiation pressure acceleration of plasma slabs by ultra-intense laser pulses were studied by 1D PIC simulations. The RR force was included via the Landau–Lifshitz approach. The numerical implementation allows the addition of RR effects to any PIC code based on the standard Boris pusher algorithm for the acceleration of the particles, at a small computational cost.

We compared the results for circular and linear polarization of the laser pulse. For CP, we found that RR effects become relevant only for plasma targets thin enough to let the laser pulse break through the foil. In this case, the inclusion of RR effects leads to an increase of the ion energy. Such an increase is, however, not very significant with respect to the case with the same laser parameters but a thicker target, for which the breakthrough of the laser pulse does not occur and RR effects are negligible.

For LP, we found that RR effects are significant, leading to some tens of per cent of energy loss by incoherent emission and to a reduction of the peak ion energy by a similar percentage. Although RR effects produce a somewhat more peaked energy spectrum during the acceleration stage, the final spectrum is in any case dominated by a post-acceleration evolution, presumably driven by high-energy electrons.

Acknowledgments

We are grateful to Dr Tatyana V. Liseykina and Professor Vitali A. Vshivkov (ICT, SD-RAS, Novosibirsk, Russia) for very useful discussions.

References

[1] Yanovsky V *et al* 2008 Ultra-high intensity 300-TW laser at 0.1 Hz repetition rate *Opt. Express* **16** 2109–14
[2] Esirkepov T, Borghesi M, Bulanov S V, Mourou G and Tajima T 2004 Highly efficient relativistic-ion generation in the laser-piston regime *Phys. Rev. Lett.* **92** 175003
[3] Bulanov S V, Echkina E Y, Esirkepov T Z, Inovenkov I N, Kando M, Pegoraro F and Korn G 2010 Unlimited ion acceleration by radiation pressure *Phys. Rev. Lett.* **104** 135003
[4] Landau L D and Lifshitz E M 1975 *The Classical Theory of Fields* 2nd edn (Oxford: Elsevier) chapter 76
[5] Zhidkov A, Koga J, Sasaki A and Uesaka M 2002 Radiation damping effects on the interaction of ultraintense laser pulses with an overdense plasma *Phys. Rev. Lett.* **88** 185002
[6] Spohn H 2000 The critical manifold of the Lorentz–Dirac equation *Europhys. Lett.* **50** 287
[7] Kostyukov I, Pukhov A and Kiselev S 2003 X-ray generation in an ion channel *Phys. Plasmas* **10** 4818
[8] Kiselev S, Pukhov A and Kostyukov I 2004 X-ray generation in strongly nonlinear plasma waves *Phys. Rev. Lett.* **93** 135004
[9] Chen M, Pukhov A, Yu T-P and Sheng Z-M 2009 Radiation reaction effects on ion acceleration in laser foil interaction arXiv:0909.5144
[10] Naumova N, Schlegel T, Tikhonchuk V T, Labaune C, Sokolov I V and Mourou G 2009 Ponderomotive ion acceleration in dense plasmas at super-high laser intensities *Eur. Phys. J.* D **55** 393–8
[11] Naumova N, Schlegel T, Tikhonchuk V T, Labaune C, Sokolov I V and Mourou G 2009 Hole boring in a DT pellet and fast-ion ignition with ultraintense laser pulses *Phys. Rev. Lett.* **102** 025002
[12] Schlegel T, Naumova N, Tikhonchuk V T, Labaune C, Sokolov I V and Mourou G 2009 Relativistic laser piston model: ponderomotive ion acceleration in dense plasmas using ultraintense laser pulses *Phys. Plasmas* **16** 083103
[13] Di Piazza A 2008 Exact solution of the Landau–Lifshitz equation in a plane wave *Lett. Math. Phys.* **83** 305
[14] Ritus V I 1985 Quantum effects of the interaction of elementary particles with an intense electromagnetic field *J. Russ. Laser Res.* **6** 497–617
[15] Walser M W and Keitel C H 2001 Geometric and algebraic approach to classical dynamics of a particle with spin *Lett. Math. Phys.* **55** 63–70
[16] Gralla S E, Harte A I and Wald R M 2009 Rigorous derivation of electromagnetic self-force *Phys. Rev.* D **80** 024031

[17] Sokolov I V, Naumova N M, Nees J A, Mourou G and Yanovsky V P 2009 Dynamics of emitting electrons in strong laser fields *Phys. Plasmas* **16** 093115

[18] Birdsall C K and Langdon A B 1991 *Plasma Physics Via Computer Simulation* (Bristol: Institute of Physics Publishing)

[19] Tamburini M *et al* 2010 Radiation reaction effects on electron nonlinear dynamics and ion acceleration in laser–solid interaction *4th Int. Conf. on Superstrong Fields in Plasmas* (*Varenna, Italy 4–9 October 2010*), *Nucl. Inst. Methods Phys. Res.* A submitted (arXiv:1011.5635)

[20] Macchi A, Veghini S, Liseykina T V and Pegoraro F 2010 Radiation pressure acceleration of ultrathin foils *New J. Phys.* **12** 045013